Analytical Biochemistry 467 (2014) 54–61

Contents lists available at ScienceDirect

Analytical Biochemistry

journal homepage: www.elsevier.com/locate/yabio

Determination of relative rate constants for in vitro RNA processing reactions by internal competition

Hsuan-Chun Lin, Lindsay E. Yandek, Ino Gjermeni, Michael E. Harris *

Department of Biochemistry, Case Western Reserve University School of Medicine, Cleveland, OH 44106, USA

ARTICLE INFO

Article history:
Received 23 June 2014
Received in revised form 8 August 2014
Accepted 20 August 2014
Available online 28 August 2014

Keywords:
Enzyme
Kinetics
Rate constant
RNA

ABSTRACT

Studies of RNA recognition and catalysis typically involve measurement of rate constants for reactions of individual RNA sequence variants by fitting changes in substrate or product concentration to exponential or linear functions. A complementary approach is determination of relative rate constants by internal competition, which involves quantifying the time-dependent changes in substrate or product ratios in reactions containing multiple substrates. Here, we review approaches for determining relative rate constants by analysis of both substrate and product ratios and illustrate their application using the in vitro processing of precursor transfer RNA (tRNA) by ribonuclease P as a model system. The presence of inactive substrate populations is a common complicating factor in analysis of reactions involving RNA substrates, and approaches for quantitative correction of observed rate constants for these effects are illustrated. These results, together with recent applications in the literature, indicate that internal competition offers an alternate method for analyzing RNA processing kinetics using standard molecular biology methods that directly quantifies substrate specificity and may be extended to a range of applications.

Quantitative comparison of rate constants for the reactions of individual RNA sequence variants is an essential experimental tool for determining the biological specificity and catalytic properties of ribozymes, ribonucleases, and RNA processing factors [1–5]. Typically, RNA substrates are analyzed one at a time by fitting time courses of changes in substrate or product concentration to linear or exponential functions to determine reaction rate constants [6–8]. This direct approach is best, but it can be time-consuming and precision may be limited by variation in enzyme-specific activity, difficulty in controlling reaction conditions between experimental trials, and inaccuracies or nonlinearity in quantification of substrate or product concentrations.

Internal competition is an alternative method for quantifying enzyme rate constants that involves analyzing the change in the ratios of concentrations of alternative substrates or products as a function of reaction progress in reactions containing multiple substrates [9–12]. This approach has potential advantages to direct fitting of kinetic data by offering higher precision, increased throughput, and less sensitivity to variation in enzyme specific activity [9,10]. Internal competition kinetics has been used extensively to measure kinetic isotope effects [12,13], and substrate and product ratios have been measured using a wide range of analytical methods, including mass spectrometry [14,15], nuclear magnetic resonance [16,17], and radioactive remote labeling [18–20]. Recently, we used linear internal competition to measure relative rate constants for in vitro transfer RNA (tRNA)[1] processing by ribonuclease P (RNase P) under initial rate (steady-state) conditions [1] and by analyzing single time-point data using equations for internal competition adapted to large substrate populations [21]. Although successful, these previous applications have not included analyses of complete reaction time courses and, importantly, have not accounted for the contributions of incomplete reacting populations of substrates or biphasic kinetics to the observed relative rate constants [22].

To provide a consistent framework for further applications of internal competition to RNA processing reactions in vitro and a resource for wider application to additional experimental systems, we briefly review approaches for the determination of relative rate constants by internal competition. Approaches for analysis of complete time courses of both precursor and product ratios for reactions containing two alternative substrates are surveyed. We demonstrate their application using the RNase P endonuclease and a two-substrate model system that allows direct comparison

* Corresponding author. Fax: +1 216 368 2110.
E-mail address: mharris@cwru.edu (M.E. Harris).

[1] *Abbreviations used:* tRNA, transfer RNA; RNase P, ribonuclease P; ptRNA, precursor tRNA; PAGE, polyacrylamide gel electrophoresis; EDTA, ethylenediaminetetraacetic acid.

http://dx.doi.org/10.1016/j.ab.2014.08.022
0003-2697/

of results with direct fitting. Importantly, an approach is described for fitting precursor ratio data to correct for inaccuracies due to inactive substrate populations. The results illustrate that internal competition provides an accurate means for quantification of specificity in RNA processing reactions with potential for improving precision and increasing throughput.

Materials and methods

Preparation of substrate ptRNA and RNase P holoenzyme

Precursor tRNAs (ptRNAs) used as substrates and the RNA subunit of the RNase P holoenzyme were generated by in vitro transcription from plasmid or polymerase chain reaction (PCR) DNA templates and purified by denaturing polyacrylamide gel electrophoresis (PAGE) as described previously [1,23,24]. The substrate ptRNAs were dephosphorylated using alkaline phosphatase and 5′ end-labeled with ^{32}P using [γ-^{32}P]ATP and polynucleotide kinase and purified using standard methods [23,25]. Concentrations of ptRNA and RNase P RNA were determined by ultraviolet (UV) spectroscopy and diluted to appropriate stock concentrations in 10 mM Tris (pH 8.0) and 1 mM ethylenediaminetetraacetic acid (EDTA).

Determination of precursor and product ratios from in vitro ptRNA processing reactions

Reaction conditions for in vitro processing of ptRNA by the RNase P holoenzyme contained 200 nM of each ptRNA, 5 nM RNase P holoenzyme, 0.1 M NaCl, 40 mM Tris (pH 8.0), 17.5 mM $MgCl_2$, and 1 mM EDTA. Mixtures containing 2× concentration of ptRNA or RNase P RNA were prepared in reaction buffer lacking $MgCl_2$ and refolded by incubation at 90 °C for 2 min. The reactions were cooled to 37 °C, the appropriate concentration of $MgCl_2$ was added, and the 37 °C incubation was continued for 30 min. An equivalent concentration of C5 protein was added to the holoenzyme solution, and the incubation was continued for an additional 15 min. Enzyme and substrate were mixed to start the reaction, and aliquots taken at appropriate time points were quenched by pipetting into an equivalent volume of 50 mM EDTA and 80% formamide.

The precursor and products from ptRNA processing reactions were resolved by PAGE on 10% acrylamide/0.5% bis-acrylamide gels containing 8 M urea. Gels were dried onto Whatman 3 MM paper, exposed to phosphorimager screens (Molecular Dynamics/GE) for 10 to 24 h, and quantified using ImageQuant software to obtain the intensities of precursor and product bands as indicated in the text. Regions of the gel outside the sample lanes were also analyzed, and the background intensity was subtracted from precursor and product band intensities. The corrected phosphorimager signals were used to compute the precursor and product ratios used in the data-fitting analyses described below.

Results and discussion

Determination of relative rate constants by internal competition

Alternative substrate kinetics is well described in the literature [9–11,26], although it is not often applied analytically to RNA processing reactions. The general equations for measurement of relative rate constants by analysis of precursor and product ratios for two alternative substrates are summarized here, and their application is illustrated. Briefly, when two substrates compete in the same reaction for association with an enzyme-active site, the ratio of their observed rates of product formation is the ratio of their respective V/K values multiplied by their concentrations [6,9,26]:

$$\frac{v_2}{v_1} = \frac{(V/K)_2}{(V/K)_1}\left(\frac{S_2}{S_1}\right). \tag{1}$$

The derivation of Eq. (1) for multiple turnover steady-state reactions is reproduced in the online supplementary material. As illustrated in Fig. 1A, S_1 and S_2 represent two alternative ptRNA substrates for the processing endonuclease RNase P, and v_1 and v_2 are the observed steady-state rates (M/s) for these two ptRNAs, respectively. The term V is the rate constant for reaction of reaction of the enzyme–substrate complex (ES) to yield free enzyme and product ($E + S$), and K is the apparent steady-state equilibrium constant (either K_d or K_m) for the multiple turnover reaction. The ratio of the V/K ($M^{-1}\,s^{-1}$) values for the two substrates provides a quantitative description of enzyme specificity [27,26] and defines a relative rate constant [$^rk = (V/K)_2/(V/K)_1$] for which the substrate included in the denominator (S_1) is considered as the reference substrate. A substrate with a larger V/K relative to the reference substrate will have an $^rk > 1$, whereas an ^rk of <1 indicates that the substrate has a correspondingly smaller V/K.

The free energy landscapes for the competitive reactions of S_1 and S_2 are illustrated in Fig. 1B. At the start of the reaction ($f = 0$), the concentrations of both substrates are at experimentally defined values, which are equimolar in this example. Similarly, after completion ($f = 1$), the ratio of products P_2/P_1 will be equivalent to the initial substrate ratio S_2/S_1 provided that all of the input substrate is active. At an intermediate time during the reaction ($f < 1$), the ratio of the substrates (S_2/S_1) and products (P_2/P_1) will be offset from their initial and final values, respectively. The faster reacting substrate, in this example S_1, becomes enriched in the product population ($P_2/P_1 > 1$) at early time points, whereas the slower reacting species is enriched in the residual unreacted substrate population ($S_2/S_1 < 1$) at later time points. These ratios change with increasing f as a function of the relative rate constant ^rk, which is defined by the differences in activation energy ($\Delta G^{\ddagger}$) for the reactions of the two substrates.

Given the following definitions for the ratios of S_1 and S_2, an expression for the ^rk can be obtained in terms of the ratios of the two substrates [11,12,28] (see supplementary material):

$$R_s = S_2/S_1$$
$$R_0 = S_{2,0}/S_{1,0}$$
$$R_p = P_2/P_1 = (S_{2,0} - S_2)/(S_{1,0} - S_1).$$

In these ratios, S_1 and S_2 are the substrate concentrations at a specific fraction of reaction (f), whereas P_1 and P_2 are the corresponding product concentrations. $S_{1,0}$ and $S_{2,0}$ are the substrate concentrations at the beginning of the reaction.

The following expression is used to quantify relative rate constants from analysis of the ratios of the concentrations of the residual unreacted substrates at a fraction of reaction (usually $f = 0.3$–0.7) sufficient to achieve a measurable level of fractionation while still providing sufficient signal:

$$^rk = \frac{\ln((1-f)R_s/R_0)}{\ln(1-f)}. \tag{2}$$

Similarly, the relative rate constant can be determined by measuring the enrichment of the faster reacting substrate in the product population at low fractions of reaction:

$$^rk = \frac{\ln\left(\left(1 - \frac{R_p}{R_0}\right)f\right)}{\ln(1-f)}. \tag{3}$$

Eqs. (2) and (3) are routinely used to measure kinetic isotope effects by analyses of multiple measurements of R_P or R_S taken at or near the f value where there will be the maximum expression of the rate difference while still providing sufficient material for analysis [12,29–32].

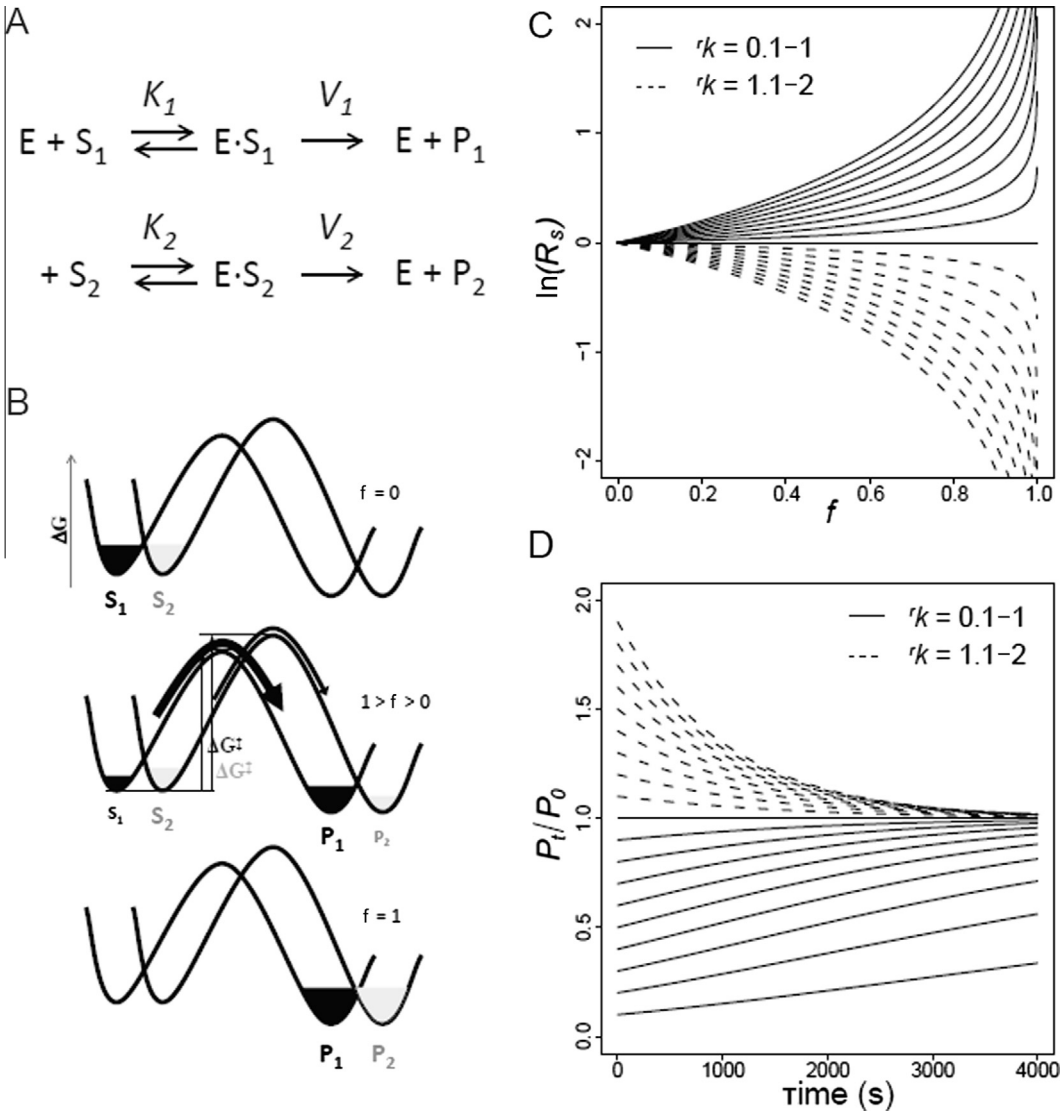

Fig.1. (A) Minimal kinetic scheme for competitive multiple turnover reactions containing two alternative substrates. A single enzyme E combines with two alternative substrates, S_1 and S_2, and reacts with rates V_1 and V_2. The equilibrium constants K_1 and K_2 are the apparent equilibrium constants (K_m or K_d) for the multiple turnover reactions of S_1 and S_2, respectively. (B) Two-dimensional free energy landscapes for the reactions of S_1 and S_2 at the start of the reaction (top, $f = 0$), at an intermediate time during the reaction (middle, $f < 1$), and after completion (bottom, $f = 1$). Note that at intermediate times during the reaction, the ratio of the substrates (S_2/S_1) and products (P_2/P_1) will be offset by their initial and final values. The relative concentrations of S_1 and S_2 are depicted in black and gray, respectively. The differences in activation energy ($\Delta G^{\ddagger}$), and consequently the differences in rate constant, are indicated y arrows. (C) Dependence of the residual substrate ratio $R_S = S_2/S_1$ as a function of reaction progress, f, for a range of normal and inverse ^{r}k values from 0.1 to 2 using Eq. (4). (D) Dependence of the residual product ratio $R_P = P_2/P_1$ as a function of time for a range of normal and inverse ^{r}k values from 0.1 to 2 using Eq. (5). Normal effects on the relative rate constant ($^{r}k > 1$) are shown by solid lines, whereas inverse effects ($^{r}k < 1$) are shown by dashed lines.

A more complete approach has been to rearrange Eq. (3) such that the measured parameters R_S and f are on opposite sides of the equation and R_0 and ^{r}k are the fitted parameters in a time course (e.g., see Refs. [12,15–17]):

$$\ln(R_s) = (^{r}k - 1)\ln(1 - f) - \ln(R_0). \tag{4}$$

In addition, the transient accumulation of the faster reacting product can be analyzed by fitting plots of R_P versus time [33]:

$$\frac{R_P}{R_0} = \frac{1 - e^{-k_2 t}}{1 - e^{-k_1 t}}. \tag{5}$$

Simulations illustrating the expected changes in precursor and product ratios for different ^{r}k values are shown in Fig. 1C and D. As the reaction proceeds, the faster reacting substrate becomes progressively depleted from the residual substrate population. Therefore, the ratio of the two substrates changes as the reaction progresses, reflecting the increasing enrichment of the slow-reacting substrate (Fig. 1C). At high fractions of reaction, even a relatively small difference in the rate constants (<2-fold) for the two substrates results in a large change in the residual substrate ratio. Similarly, the ratio of the two products shows characteristic changes as a function of reaction progress, depending on the relative rate constant. In this case, the fast-reacting substrate is enriched at early time points and the product ratio approaches the initial substrate ratio as the reaction progresses (Fig. 1D).

As described below, for RNA processing reactions, the presence of unreactive misfolded substrate populations is a potential complicating factor. In this case, the concentration of S_2 can be given by

$$S_2 = S_{2,0}(1 - U_2)e^{-k_2 t} + S_{2,0}U_2, \tag{6}$$

where U_2 is the fraction of substrate population S_2 that is inactive for processing by the enzyme and $S_{2,0}$ is the initial substrate

concentration. For the reference substrate, the reaction kinetics is assumed to be ideal:

$$S_1 = S_{1,0}(e^{-k_1 t}). \quad (7)$$

If the concentrations of the two substrates are essentially equal, then the ratios of the two substrates become the following (see supplementary material):

$$\frac{S_2}{S_1} = (1 - U_2)(1 - f)^{({}^{r}k-1)} + \frac{U_2}{(1-f)}. \quad (8)$$

This form can then be used to fit substrate ratio data in order to determine the experimental ${}^{r}k$ value when the fraction of the experimental substrate that has a known fraction, U_2, is unreactive as illustrated below. It is also possible for there to be a fraction of the reference substrate population (U_1) that is inactive as well. As illustrated below, a significant U_1 value results in an apparent increase in the calculated ${}^{r}k$ from fitting to Eq. (8), whereas the ${}^{r}k$ value decreases as U_2 increases. As a consequence, data fitting using equations in which both U_1 and U_2 are variables proved to be problematic due to difficulty in specifying the relative magnitudes of these parameters. Note that no assumption is made regarding the size of the fraction of inactive fraction U; thus, Eq. (8) is general. However, as the active fraction of the experimental substrate population decreases, the signal/noise ratio will also decrease and ultimately place a limit on the size of the unreactive population that can be analyzed.

With respect to practical application of competitive alternative substrate kinetics for structure–function experiments, several key issues follow from application of this approach [9–11]. First, because both substrates must compete for the available free enzyme in order to react and form product, the association step contributes to the relative population of ES_1 and ES_2 and, therefore, the observed rates. Direct measurements of rate constants, therefore, is the only way to determine ${}^{r}k$ values for V. However, if V reflects the same rate constant as that measured under single turnover conditions ($E \gg S$), then it should be possible to measure relative effects on V by internal competition kinetics performed under these conditions. Second, because the enzyme concentration occurs in the rate equations for v_{obs1} and v_{obs2}, it cancels out in their ratio. So long as the steady-state conditions are maintained, the ratio of observed rates and the ratio of V/K values are independent of enzyme concentration. This could be useful for reactions involving impure enzyme or difficult-to-control reaction conditions. Third, it is also evident that the individual step or steps in the reaction scheme that is rate limiting for V/K does not need to be the same for the two substrates. Application of competitive kinetics, therefore, will report on the relative V/K values for the two substrates, and provided that the V/K of the reference substrates is known, the other can be calculated but does not make any assumptions about what is rate limiting for either substrate. Fourth, because substrate and product ratios are analyzed, systematic errors in the accuracy of their measurement such as differences in enzyme-specific activity or reaction conditions or inaccuracies in measurements of substrate or product concentrations (i.e., differences in species ionization during mass spectrometry analysis), which confound direct data fitting, cancel out in the internal competition approach, and this can result in a corresponding increase in precision of relative rate constant measurements.

In vitro processing of alternative ptRNA substrates by RNase P

In vitro processing of ptRNA processing by RNase P is a good model system to examine the advantages and disadvantages of using internal competition kinetics for in vitro RNA processing reactions, including ribozyme catalysis. RNase P is a ribonucleoprotein enzyme that cleaves ptRNA to generate the mature tRNA 5′ end. Typical in vitro RNA processing reactions, such as those used to measure RNase P activity, use radiolabeled RNA, and the substrate and products are resolved by PAGE. The absolute intensities of the resulting bands are quantified by phosphorimager analysis. Structure–function studies in vitro have been used to gain insight into the intrinsic molecular recognition properties of RNase P that determine its biological function [34,35]. Endogenous ptRNA substrates have similar V/K values; however, changes in sequence and structure contacted by RNase P can result in miscleavage or reduced processing rate constants [1,21]. Thus, RNase P is a useful example for application of internal competition that is relevant to a wider range of RNA processing reactions and enzyme systems.

To apply internal competition kinetic analyses, it is necessary to measure the ratio of the concentrations of the two competing substrates or products and to precisely measure the fraction of reaction of the reference substrate [11]. As shown in Fig. 2A, the ptRNA^{Met} substrate has a 5′ leader sequence that is 10 nt in length, whereas the ptRNA^{Met}L1+21 and ptRNA^{Met}L5+21 substrates have leader sequences that are 31 nt long. In addition, these substrates differ from ptRNA^{Met} at positions N(−3) to N(−8) relative to the cleavage site that is located between nucleotides N(−1) and N(1). These positions contact or influence the binding to the essential protein cofactor in the RNase P–ptRNA complex, and variation of their sequence affects the observed V/K value for processing by *Escherichia coli* RNase P [21]. The difference in 5′ leader length allows the precursors and products of both substrates to be resolved by PAGE and, thus, allows time courses for their reactions to be analyzed separately by fitting these data to an exponential function (Fig. 3A and B). Consistent with previous results, the ptRNA^{Met} substrate with the L5+21 leader sequence (ptRNA^{Met}L5+21) is processed with an

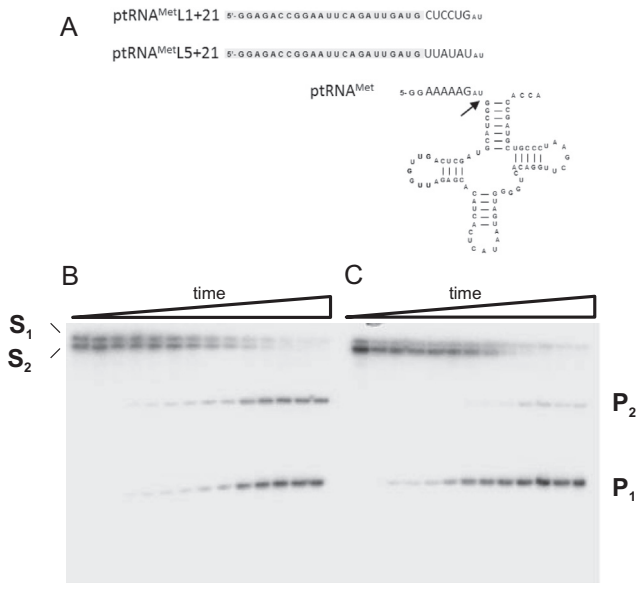

Fig.2. Quantification of substrate and product ratios for in vitro RNase P reactions containing two alternative ptRNA substrates. (A) Sequence and secondary structure of the reference substrate ptRNA^{Met} (i.e., S_1) and two experimental substrates ptRNA^{Met}L1+21 and ptRNA^{Met}L5+21 (i.e., S_2). These three substrates differ in nucleotides N(−6) to N(−3), numbering relative to the RNase P cleavage site between N(−1) and N(1). These sequences are within the binding site for the essential RNase P protein, and variation can affect the V/K for individual substrates. (B) PAGE analysis of the precursor and products of in vitro RNase P reaction containing the ptRNA^{Met} and ptRNA^{Met}L1+21 substrates. (C) PAGE analysis of the precursor and products of in vitro RNase P reaction containing the ptRNA^{Met} and ptRNA^{Met}L5+21 substrates. The positions of the substrates and products in the gel are indicated. Quantification of these data by phosphorimager analysis is used to determine S_2/S_1 and P_2/P_1 ratios analyzed in Fig. 3.

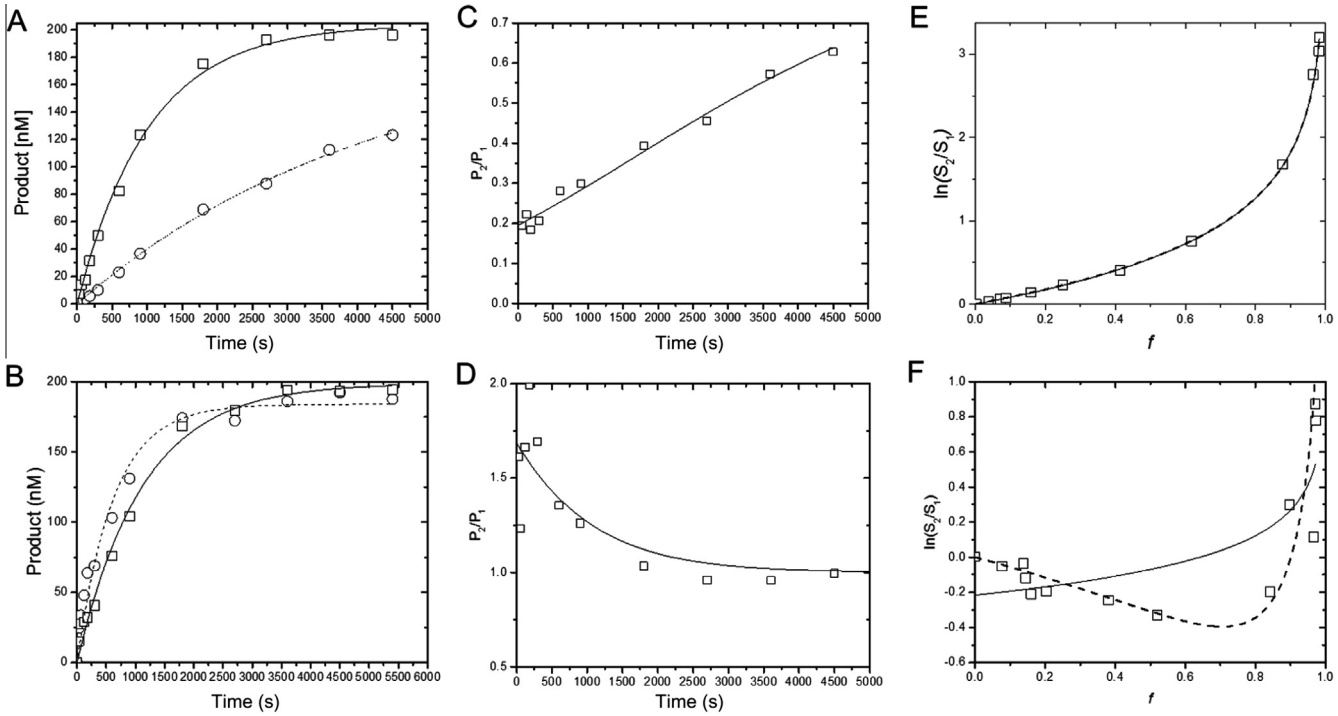

Fig.3. Determination of rate constants for the ptRNA^{Met}L1+21 and ptRNA^{Met}L5+21 substrates by direct fitting and internal competition analysis of substrate and product ratios. (A) Kinetic data for product accumulation in individual reactions containing either ptRNA^{Met} (squares, solid line) or ptRNA^{Met}L5+21 (circles, dashed line). (B) Kinetic data for product accumulation in individual reactions containing either ptRNA^{Met} (squares, solid line) or ptRNA^{Met}L1+21 (circles, dashed line). The data in panels A and B are fit to a single exponential function to obtain k_{obs}. (C,D) Plots of the product ratio data from the reactions of ptRNA^{Met}L5+21 and ptRNA^{Met} [$(P_2/P_1$ = ptRNA^{Met}L1+21/ptRNA^{Met}) versus f] (C) and of ptRNA^{Met}L1+21 and ptRNA^{Met} [$(P_2/P_1$ = ptRNA^{Met}L5+21/ptRNA^{Met}) versus f] (D). These data are fit to Eq. (5) (solid line) to determine the relative rate constants for the ptRNA^{Met}L1+21 and ptRNA^{Met}L5+21 substrates. (E,F). Plots of the substrate ratio data from the reactions of ptRNA^{Met}L5+21 and ptRNA^{Met} [$(S_2/S_1$ = ptRNA^{Met}L1+21/ptRNA^{Met}) versus f] (E) and of ptRNA^{Met}L1+21 and ptRNA^{Met} [$(S_2/S_1$ = ptRNA^{Met}L5+21/ptRNA^{Met}) versus f] (F). The data in both panels are fit to Eq. (4) (solid lines) to determine the relative rate constants for the ptRNA^{Met}L1+21 and ptRNA^{Met}L5+21 substrates. The data in panel F are also fit to Eq. (8) (dashed line) assuming a U value of 0.062 to account for the increase in the S_2/S_1 ratio at higher fractions of reaction. Averages and standard deviations of the rate constants for all three substrates are summarized in Table 1.

Table 1
Comparison of relative reaction rate constants determined by direct fitting and internal competition using either product or substrate ratios.

	k_{obs} min^{-1}	Direct fitting ^{r}k (calc.)[a]	Product ratio ^{r}k	Substrate ratio	
				^{r}k	^{r}k (corr.)[b]
ptRNA^{Met}	0.0006(3)				
ptRNA^{Met}L1+21	0.0010(5)	1.8 (9)	1.4 (2)	0.9 (1)	1.6 (5)
ptRNA^{Met}L5+21	0.00017(4)	0.24 (5)	0.30 (4)	0.22 (1)	0.22 (2)

[a] Relative rate constants calculated from k_{obs} values. Standard deviations are shown in parentheses, and errors on calculated ^{r}k values are propagated accordingly.
[b] Corrected ^{r}k values obtained by fitting to Eq. (8).

approximately 4-fold slower rate constant at 0.00017 min^{-1} compared with the reference substrate that reacted with an observed rate constant of 0.0006 min^{-1} (Table 1). Calculation of a relative rate constant from these values yields a value of ^{r}k = 0.14(5). The ptRNA^{Met}L1+21 substrate with the L1+21 leader sequence shows an approximately 2-fold faster rate constant (0.0010 min^{-1}) relative to ptRNA^{Met} yielding a calculated ^{r}k value of 1.8(9) using the rate constants measured by direct fitting; however, in these experiments the propagated error from the individual measurements is relatively large, placing an intrinsic limit on any mechanistic interpretation that may be drawn.

Determination of relative rate constants by analysis of substrate and product ratios

The ^{r}k values for substrate and product ratios were also determined by fitting the data from experiments exemplified in Fig. 2A and B to Eqs. (4) and (5). As shown in Fig. 3C, the ratio of the products for the reaction containing ptRNA^{Met}L5+21 and ptRNA^{Met} expressed as $R_P = P_2/P_1$ = ptRNA^{Met}L5+21/ptRNA^{Met} (i.e., using ptRNA^{Met} as the reference substrate) showed a transient depletion due to accumulation of the product from the faster reacting ptRNA^{Met} species at early time points. In contrast, there is a transient enrichment of the ptRNA^{Met}L1+21 product and a corresponding larger ptRNA^{Met}L1+21/ptRNA^{Met} product ratio at early time points (Fig. 3D). Fitting these data to Eq. (5) yielded absolute values for k_1 and k_2 that were used to calculate ^{r}k values of 1.4(2) for ptRNA^{Met}L1+21 and 0.30(4) for ptRNA^{Met}L5+21 that compare favorably with the results from direct fitting (Table 1).

A large increase is observed in the ptRNA^{Met}L5+21/ptRNA^{Met} ratio ($R_S = S_2/S_1$) as the reaction containing both substrates proceeds due to the larger rate constant for ptRNA^{Met} and the faster depletion of this substrate from the residual substrate population (Fig. 3E). Fitting these data to Eq. (4) yielded an ^{r}k value of 0.22(1), consistent with both direct fitting and internal competition analysis of product ratios (Table 1). However, as shown in Fig. 3F, the change in substrate ratio (ptRNA^{Met}L1+21/ptRNA^{Met} = S_2/S_1) as a function of reaction progress does not follow ideal

behavior for the reaction containing ptRNA^{Met}L1+21 and ptRNA^{Met} substrates. In this case, an initial decrease in the ptRNA^{Met}L1+21/ptRNA^{Met} ratio is observed, followed by an increase at later time points. The non-ideal behavior is likely due to misfolding of a portion of the ptRNA^{Met}L1+21 substrate RNA population that renders it refractory to cleavage by RNase P. This behavior is not unexpected given that a characteristic feature of the biophysical behavior of structured RNAs is their ability to adopt alternative folded structures [22,36]. Only one or a subset of these alternative structures may be biologically active, and examples where this has been observed include tRNA folding (see Ref. [22] and references therein). Indeed, the data in Fig. 2B show that a small fraction of residual ptRNA^{Met}L1+21 substrate is not consumed.

To illustrate the effect of substrate misfolding resulting in inactive species in the experimental sample, we simulated the substrate ratio data for hypothetical substrates with slower ($^{r}k = 0.5$) or faster ($^{r}k = 2$) rate constants than the reference substrate or with the same rate constant ($^{r}k = 1$) using Eq. (6). For each case, the effect of increasing fraction of unreactive experimental substrate, U_2, on the observed S_2/S_1 ratio was simulated ranging from 0.01 to 0.1 using the exponential functions in Eqs. (6) and (7) (Fig. 4A). When $^{r}k = 0.5$ and the observed S_2/S_1 data are fit to Eq. (4), which assumes complete reaction of both S_1 and S_2, an increasingly inaccurate ^{r}k value is obtained for the reaction of S_2 as the fraction of unreactive population increases. For a reaction where there is no difference in the rate constants for the two substrates ($^{r}k = 1$), the presence of unreactive species in the experimental substrate population results in an apparent increase in the S_2/S_1 ratio and $^{r}k < 1$ is obtained from fitting to Eq. (4). Although this effect is comparatively small, it is apparent that an experimental substrate that has no difference in rate constant relative to the reference substrate ($^{r}k = 1$) could be subject to false interpretation that it reacts more slowly if an appreciable fraction is misfolded and, therefore, inactive. For an experimental substrate that reacts with a faster rate constant than the reference ($^{r}k = 2$), the S_2/S_1 ratio decreases as the reaction proceeds; however, increasing fractions of unreactive S_2 result in deflection of this trend and ultimately an overall increase in the S_2/S_1 ratio (Fig. 4B). As a result, fitting these data to Eq. (4) returns an increasingly inaccurate ^{r}k value that underestimates the intrinsic value (Fig. 4D). Thus, the presence of unreactive species in the experimental substrate population can significantly confound internal competition analyses of substrate ratios.

As illustrated in Fig. 3F, for the reaction containing both ptRNA^{Met}L5+21 and ptRNA^{Met} substrates, the data are adequately described by a function describing a faster reacting S_2 that also contains a small fraction that is inactive (Eq. (8)). The derivation of Eq. (8) is provided in the supplementary material and includes the variable, U_2, for the fraction of the experimental substrate that is unreactive. An ^{r}k value of 1.6(5) is obtained by fitting to this function and a U_2 value of 0.03, consistent with the PAGE data observed in Fig. 2B. It is also possible that there will be an unreactive fraction in the reference substrate (U_1) as well as an unreactive fraction in the experimental substrate (U_2). To explore the consequences of this scenario, we performed a series of simulations for $^{r}k = 2$ in which U_1 was assumed to be 0.1 and U_2 was varied from 0 to 0.1 (Fig. 4C). A significant fraction of unreacted reference substrate U_1 results in an artificially lower S_2/S_1 substrate ratio at high fractions of reaction that results in an overestimate of the intrinsic ^{r}k value. This result contrasts with the effect of increased U_2 values that result in an underestimate of the intrinsic ^{r}k (Fig. 4D). Although an expression containing both U_1 and U_2 as variables can be derived, data fitting proved to be problematic due to the opposing effects of their values on the observed S_2/S_1 ratio. A more

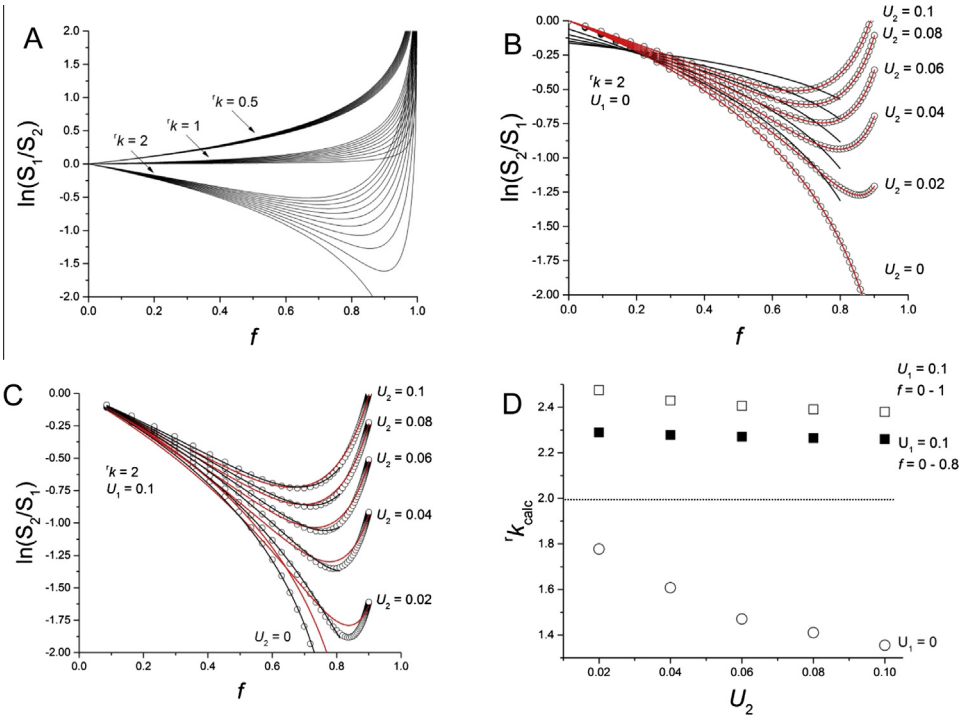

Fig.4. Effects of increasing unreactive substrate population (U) on the observed change in substrate ratio (S_2/S_1) as a function of reaction progress (f). (A) Simulations of S_2/S_1 as a function of f for substrates with $^{r}k = 0.5$, 1, and 2. At each ^{r}k value, the magnitude of U was varied from 0.01 to 0.1. (B) Detail showing the simulated data from panel A for the case of $^{r}k = 2$ with increasing U from 0 to 0.1 as indicated. The data for conversion of 80% of the substrate ($f = 0$–0.8) were fit to Eq. (4) (shown in black) to obtain apparent ^{r}k values as summarized in panel D. These data were also fit to Eq. (8) (shown in red), which accurately describes the data and, therefore, returns accurate ^{r}k values. (C) Simulations showing the effect of the presence of unreactive populations in both the substrate (U_2) and the reference substrate (U_1). The U_1 value was fixed at 0.1 and U_2 was varied from 0.02 to 0.1 as indicated. These simulated data were fit to Eq. (8) either using the entire data set or restricted to $f < 0.8$. (D) Summary of calculated ^{r}k values ($^{r}k_{calc}$) from fitting simulated data in panels B and C. The values of $^{r}k_{calc}$ from fitting the simulated data in panel B to Eq. (4) (open circles), the entire range of data in panel C to Eq. (8), and the data for $f < 0.8$ from panel C to Eq. (8) (filled squares) are shown as a function of U_2.

general solution is to fit these data with Eq. (8) in which a single value for the experimental substrate is assumed. As shown in Fig. 4C and D, fitting the entire time course returns ^{r}k values that overestimate the intrinsic value by as much as 25% (~2.5–2.4 vs. 2.0). However, when the fitting is restricted to $f < 0.8$, the calculated ^{r}k value is more accurate (~2.2–2.0). Therefore, in cases where analysis of product ratios is not applicable, and there is a significant (and unavoidable) fraction of the experimental and reference substrates that is unreactive, it is nonetheless possible to obtain accurate relative rate constants.

Conclusions

Direct fitting of kinetic data is the primary tool of enzyme kinetics, including RNA processing enzymes and ribozymes; however, internal competition can offer significant advantages in some cases and can serve as a valuable experimental tool. As illustrated by the examples presented here, this approach can be used to accurately distinguish small differences in relative rate constants for reactions of alternative RNA substrates in vitro. The ability to compare reaction kinetics within the same reaction necessarily minimizes differences due to enzyme concentration and specific activity. Thus, competitive methods may be particularly useful for complex enzyme preparations or extracts. Importantly, alternative substrate kinetics provides a direct readout of enzyme specificity that is essential for understanding the competition between substrates in vivo [1,20,37]. The method is applicable to single time-point assays in those cases where the entire reaction course cannot be followed or material is limiting. However, fitting of multiple data points over reaction time courses is preferable for optimizing accuracy. Internal competition kinetics is also advantageous when measuring absolute substrate concentrations is difficult, for example, in mass spectrometry where differences in ionization can influence signal intensities. Because changes in substrate or product ratios are quantified, inaccuracies in their values cancel [e.g., $R_S/R_0 = (S_2/S_1)/(S_{2,0}/S_{1,0}) = (S_2/S_{2,0})/(S_1/S_{1,0})$], with concomitant increases in accuracy of rate constant measurements [11,38]. As noted previously in the literature on kinetic isotope effect (KIE) analyses by internal competition, there are inherent limitations due to low signal-to-noise ratios at early and late fractions of reaction [12]. That is, at low fractions of reaction there is little change in the residual substrate ratio, whereas at high fractions of reaction the enrichment of the slower reacting substrate is greatest. However, this increase in fractionation is offset by inaccuracy in measuring the remaining low concentration of unreacted substrate. In addition, the results shown here further underscore the limitation that small differences in inactive populations can be problematic for quantifying small differences in rate constants. Purification of substrate RNAs by non-denaturing PAGE to isolate more uniformly folded population could provide a way to avoid this limitation. Nonetheless, the approach is broadly applicable, and advantages include the ability to quantify effects on reaction rate constants with greater precision, increased throughput of individual kinetic trials, and the potential to recognize non-ideal kinetic behavior. The simple kinetic method applied here provides a consistent framework for extending internal competition analysis to other systems and more complex substrate populations.

Acknowledgments

We thank Vernon Anderson for assistance and advice on application of competitive methods and thank members of the Harris laboratory for comments on the manuscript. The diagrams illustrating internal competition in Fig. 1B were adapted from images provided by Mark Ruszczycky. This work was supported by National Institutes of Health (NIH) grants GM096000 and GM056740 to M.E.H.

Appendix A. Supplementary data

Supplementary data associated with this article can be found, in the online version, at http://dx.doi.org/10.1016/j.ab.2014.08.022.

References

[1] L.E. Yandek, H.C. Lin, M.E. Harris, Alternative substrate kinetics of *Escherichia coli* ribonuclease P: determination of relative rate constants by internal competition, J. Biol. Chem. 288 (2013) 8342–8354.
[2] T. Dale, R.P. Fahlman, M. Olejniczak, O.C. Uhlenbeck, Specificity of the ribosomal A site for aminoacyl-tRNAs, Nucleic Acids Res. 37 (2009) 1202–1210.
[3] D.A. Cooper, B.K. Jha, R.H. Silverman, J.R. Hesselberth, D.J. Barton, Ribonuclease L and metal-ion-independent endoribonuclease cleavage sites in host and viral RNAs, Nucleic Acids Res. 42 (2014) 5202–5216.
[4] J. Hougland, J. Piccirilli, M. Forconi, J. Lee, D. Herschlag, How the group I intron works: a case study of RNA structure and function, in: R. Akins, R. Gesteland, T. Cech (Eds.), The RNA World, third ed., Cold Spring Harbor Laboratory Press, Cold Spring Harbor, NY, 2006.
[5] A.W. Nicholson, Ribonuclease III mechanisms of double-stranded RNA cleavage, Wiley Interdiscip. Rev. RNA 5 (2014) 31–48.
[6] A. Fersht, Structure and Mechanism in Protein Science, W. H. Freeman, San Francisco, 1998.
[7] W.W. Cleland, P.F. Cook, Enzyme Kinetics and Mechanism, Garland, New York, 2007.
[8] O.C. Uhlenbeck, Keeping RNA happy, RNA 1 (1995) 4–6.
[9] S. Cha, Kinetics of enzyme reactions with competing alternative substrates, Mol. Pharmacol. 4 (1968) 621–629.
[10] V. Schellenberger, R.A. Siegel, W.J. Rutter, Analysis of enzyme specificity by multiple substrate kinetics, Biochemistry 32 (1993) 4344–4348.
[11] W.W. Cleland, The use of isotope effects to determine enzyme mechanisms, Arch. Biochem. Biophys. 433 (2005) 2–12.
[12] L. Melander, W.H. Saunders Jr., Reaction Rates of Isotopic Molecules, John Wiley, New York, 1980.
[13] A. Kohen, H.H. Limbach, Isotope Effects in Chemistry and Biology, Taylor & Francis/CRC, Boca Raton, FL, 2005.
[14] N. Pi, J.A. Leary, Determination of enzyme/substrate specificity constants using a multiple substrate ESI–MS assay, J. Am. Soc. Mass Spectrom. 15 (2004) 233–243.
[15] M.E. Harris, Q. Dai, H. Gu, D.L. Kellerman, J.A. Piccirilli, V.E. Anderson, Kinetic isotope effects for RNA cleavage by 2′-O-transphosphorylation: nucleophilic activation by specific base, J. Am. Chem. Soc. 132 (2010) 11613–11621.
[16] K.A. Manning, B. Sathyamoorthy, A. Eletsky, T. Szyperski, A.S. Murkin, Highly precise measurement of kinetic isotope effects using ^{1}H-detected 2D [^{13}C,^{1}H]-HSQC NMR spectroscopy, J. Am. Chem. Soc. 134 (2012) 20589–20592.
[17] J. Chan, A.R. Lewis, M. Gilbert, M.F. Karwaski, A.J. Bennet, A direct NMR method for the measurement of competitive kinetic isotope effects, Nat. Chem. Biol. 6 (2010) 405–407.
[18] D.A. Hiller, M. Zhong, V. Singh, S.A. Strobel, Transition states of uncatalyzed hydrolysis and aminolysis reactions of a ribosomal P-site substrate determined by kinetic isotope effects, Biochemistry 49 (2010) 3868–3878.
[19] D.W. Parkin, H.B. Leung, V.L. Schramm, Synthesis of nucleotides with specific radiolabels in ribose: primary ^{14}C and secondary ^{3}H kinetic isotope effects on acid-catalyzed glycosidic bond hydrolysis of AMP, dAMP, and inosine, J. Biol. Chem. 259 (1984) 9411–9417.
[20] J.G. Bertram, K. Oertell, J. Petruska, M.F. Goodman, DNA polymerase fidelity: comparing direct competition of right and wrong dNTP substrates with steady state and pre-steady state kinetics, Biochemistry 49 (2010) 20–28.
[21] U.P. Guenther, L.E. Yandek, C.N. Niland, F.E. Campbell, D. Anderson, V.E. Anderson, M.E. Harris, E. Jankowsky, Hidden specificity in an apparently nonspecific RNA-binding protein, Nature 502 (2013) 385–388.
[22] D. Herschlag, RNA chaperones and the RNA folding problem, J. Biol. Chem. 270 (1995) 20871–20874.
[23] D. Siew, N.H. Zahler, A.G. Cassano, S.A. Strobel, M.E. Harris, Identification of adenosine functional groups involved in substrate binding by the ribonuclease P ribozyme, Biochemistry 38 (1999) 1873–1883.
[24] J.L. Brunelle, R. Green, In vitro transcription from plasmid or PCR-amplified DNA, Methods Enzymol. 530 (2013) 101–114.
[25] R. Porecha, D. Herschlag, RNA radiolabeling, Methods Enzymol. 530 (2013) 255–279.
[26] D. Herschlag, The role of induced fit and conformational changes of enzymes in specificity and catalysis, Bioorg. Chem. 16 (1988) 62–96.
[27] D.B. Northrop, Rethinking fundamentals of enzyme action, Adv. Enzymol. Relat. Areas Mol. Biol. 73 (1999) 25–55.
[28] W.W. Cleland, Use of isotope effects to elucidate enzyme mechanisms, CRC Crit. Rev. Biochem. 13 (1982) 385–428.

[29] D.J. Merkler, P.C. Kline, P. Weiss, V.L. Schramm, Transition-state analysis of AMP deaminase, Biochemistry 32 (1993) 12993–13001.
[30] G.A. Sowa, A.C. Hengge, W.W. Cleland, ^{18}O isotope effects support a concerted mechanism for ribonuclease A, J. Am. Chem. Soc. 119 (1997) 2319–2320.
[31] A.C. Hengge, J.M. Denu, J.E. Dixon, Transition-state structures for the native dual-specific phosphatase VHR and D92N and S131A mutants: contributions to the driving force for catalysis, Biochemistry 35 (1996) 7084–7092.
[32] D.A. Hiller, V. Singh, M. Zhong, S.A. Strobel, A two-step chemical mechanism for ribosome-catalysed peptide bond formation, Nature 476 (2011) 236–239.
[33] P.J. Unrau, D.P. Bartel, An oxocarbenium–ion intermediate of a ribozyme reaction indicated by kinetic isotope effects, Proc. Natl. Acad. Sci. U.S.A. 100 (2003) 15393–15397.
[34] J.K. Smith, J. Hsieh, C.A. Fierke, Importance of RNA–protein interactions in bacterial ribonuclease P structure and catalysis, Biopolymers 87 (2007) 329–338.
[35] R.K. Hartmann, M. Gossringer, B. Spath, S. Fischer, A. Marchfelder, The making of tRNAs and more—RNase P and tRNase Z, Prog. Mol. Biol. Transl. Sci. 85 (2009) 319–368.
[36] R. Russell, RNA misfolding and the action of chaperones, Front. Biosci. 13 (2008) 1–20.
[37] S. Ledoux, O.C. Uhlenbeck, Different aa–tRNAs are selected uniformly on the ribosome, Mol. Cell 31 (2008) 114–123.
[38] A.G. Cassano, B. Wang, D.R. Anderson, S. Previs, M.E. Harris, V.E. Anderson, Inaccuracies in selected ion monitoring determination of isotope ratios obviated by profile acquisition: nucleotide $^{18}O/^{16}O$ measurements, Anal. Biochem. 367 (2007) 28–39.